Since January 2020 Elsevier has created a COVID-19 resource centre with free information in English and Mandarin on the novel coronavirus COVID-19. The COVID-19 resource centre is hosted on Elsevier Connect, the company's public news and information website.

Elsevier hereby grants permission to make all its COVID-19-related research that is available on the COVID-19 resource centre - including this research content - immediately available in PubMed Central and other publicly funded repositories, such as the WHO COVID database with rights for unrestricted research re-use and analyses in any form or by any means with acknowledgement of the original source. These permissions are granted for free by Elsevier for as long as the COVID-19 resource centre remains active.

Journal of Neuroscience Methods 285 (2017) 58–68

Contents lists available at ScienceDirect

Journal of Neuroscience Methods

journal homepage: www.elsevier.com/locate/jneumeth

Research paper

An optimized method for enumerating CNS derived memory B cells during viral-induced inflammation

Krista D. DiSano[a,b], Stephen A. Stohlman[a,1], Cornelia C. Bergmann[a,*]

[a] Department of Neurosciences NC30, Lerner Research Institute, Cleveland Clinic Foundation, 9500 Euclid Avenue, Cleveland, OH 44195, United States
[b] School of Biomedical Sciences, Kent State University, Kent, OH 44242, United States

HIGHLIGHTS

- Memory B cell markers characterizing peripheral B cell phenotypes show more diverse expression patterns in the infected central nervous system (CNS).
- TLR7/8 stimulation for 2 days prior to ELISPOT analysis achieves optimal conversion of CNS-derived memory B cells to ASC while minimizing cell loss.
- *In vitro* stimulation allows simultaneous assessment of antibody secreting cell and memory B cell isotype, antigen specificity, and temporal alterations during CNS inflammation.

ARTICLE INFO

Article history:
Received 26 January 2017
Received in revised form 26 April 2017
Accepted 7 May 2017
Available online 8 May 2017

Keywords:
Memory B cells
Central nervous system
Virus infection
Antibody secreting cells

ABSTRACT

Background: CNS inflammation resulting from infection, injury, or neurodegeneration leads to accumulation of diverse B cell subsets. Although antibody secreting cells (ASC) within the inflamed CNS have been extensively examined, memory B cell (Bmem) characterization has been limited as they do not secrete antibody without stimulation. Moreover, unlike human Bmem, reliable surface markers for murine Bmem remain elusive.

New method: Using a viral encephalomyelitis model we developed a modified limiting dilution *in vitro* stimulation assay to convert CNS-derived virus specific Bmem into ASC.

Comparison with existing methods: Stimulation methods established for lymphoid tissue cells using prolonged stimulation with viral lysate resulted in substantial ASC loss and minimal Bmem to ASC conversion of CNS-derived cells. By varying stimulation duration, TLR activators, and culture supplements, we achieved optimal conversion by culturing cells with TLR7/8 agonist R848 in the presence of feeder cells for 2 days.

Results: Flow cytometry markers CD38 and CD73 characterizing murine Bmem from lymphoid tissue showed more diverse expression patterns on corresponding CNS-derived B cell subsets. Using the optimized TLR7/8 stimulation protocol, we compared virus-specific IgG Bmem *versus* pre-existing ASC within the brain and spinal cord. Increasing Bmem frequencies during chronic infection mirrored kinetics of ASC. However, despite initially similar Bmem and ASC accumulation, Bmem prevailed in the brain, but were lower than ASC in the spinal cord during persistence.

Conclusion: Simultaneous enumeration of antigen-specific Bmem and ASC using the Bmem assay optimized for CNS-derived cells enables characterization of temporal changes during microbial or autoantigen induced neuroinflammation.

© 2017 Elsevier B.V. All rights reserved.

1. Introduction

Antibody (Ab) secreting cells (ASC) and serum Ab are essential immune components that neutralize pathogens during infection and mediate protective immunity following vaccination. However, serum immunoglobulin (Ig) is short-lived lasting several weeks and requires continuous production to maintain protective immunity for years or even life of the host (Slifka and Ahmed, 1996a; Slifka et al., 1998). The production of serum Ab is sustained not only by long-lived fully differentiated ASC, termed plasma cells which reside in the bone marrow, but also by memory B cells (Bmem) that can rapidly convert to ASC (Slifka et al., 1998; Kurosaki et al., 2015). Bmem arise both during germinal center (GC) dependent

* Corresponding author.
E-mail address: bergmac@ccf.org (C.C. Bergmann).
[1] Deceased.

http://dx.doi.org/10.1016/j.jneumeth.2017.05.011
0165-0270/© 2017 Elsevier B.V. All rights reserved.

(IgG^+ Bmem) or independent responses (IgM^+ Bmem) following initial antigen exposure and can persist independent of antigen within secondary lymphoid tissue (SLT) for years (Kurosaki et al., 2015; Taylor et al., 2012). Although Bmem do not spontaneously secrete Ab, minimal stimulation requirements, including T cell help and/or secondary encounter of antigen can trigger rapid differentiation into antigen-specific ASC or re-seed GC, thereby promoting isotype switching and somatic hypermutation (Kurosaki et al., 2015; Zuccarino-Catania et al., 2014; Pape et al., 2011; Dogan et al., 2009; Hebeis et al., 2004; Aiba et al., 2010). In addition to contributing to long-lived humoral immunity, Bmem function as potent antigen presenting cells and as immune modulators by secreting cytokines (Shimoda and Koni, 2007; Duddy et al., 2007; Adlowitz et al., 2015; Lund, 2008; Lino et al., 2016). Although studies of B cells within the inflamed CNS have commonly focused on ASC and Ab specificity, B cell populations accumulating during CNS infection, injury, and neurodegeneration are diverse and include Bmem (Duddy et al., 2007; Niino et al., 2009; Krumbholz et al., 2012; Michel et al., 2015; Metcalf and Griffin, 2011; Cepok et al., 2006; Phares et al., 2014; Dang et al., 2015; Ankeny et al., 2009). However, the role of Bmem within the inflamed CNS is relatively unexplored due to limitations of reliable surface markers, particularly in murine models.

Human Bmem are classically distinguished by expression of CD27, a protein belonging to the tumor necrosis factor receptor (TNFR) family that provides signals regulating entry into plasma cell lineage (Klein et al., 1998; Tangye et al., 1998). More detailed human Bmem phenotyping revealed heterogeneous populations, including $CD27^-$ Bmem, and markers have expanded to include specific patterns of CD38, CD21, CD24, CD19, B220, FcRH4 and CD25 (Amu et al., 2007; Küppers, 2008; Sanz et al., 2008). While this panel has aided in identifying several reliable markers of human Bmem, murine Bmem characterization is limited by the low frequency of Bmem and minimal expression of CD27 (Xiao et al., 2004; Anderson et al., 2007; Liu et al., 1996; Ridderstad and Tarlinton, 1998). Although several markers including CD73, CD38, CD80 and PD-L2 have been proposed to define at least five subsets of Bmem, these markers are also expressed by several other B cell phenotypes within SLT (Zuccarino-Catania et al., 2014; Anderson et al., 2007; Conter et al., 2014; Tomayko et al., 2010). Moreover, our own studies of murine B cell subsets in the central nervous system (CNS) have revealed unique patterns of activation markers compared to peripheral B cell counterparts, further complicating identification of CNS B cell subsets based on well-defined SLT markers (DiSano et al., 2017). For example, CD80, a marker of CD4T cell help and a proposed marker defining subpopulations of Bmem within SLT, was found on multiple B cell phenotypes within the CNS (DiSano et al., 2017). Bmem analysis *in vivo* has largely relied on protein immunizations in B cell receptor (BCR) transgenic mice to increase Bmem frequencies, or on antigenic challenge in naïve recipients of adoptively transferred antigen-specific B cells. Both *in vitro* and *in vivo* Bmem to ASC conversion has been shown to require proliferation (Slifka and Ahmed, 1996b; Cao et al., 2010; Pinna et al., 2009; Tangye and Hodgkin, 2004; Bernasconi et al., 2002; Kometani et al., 2013). Quantitative assessment of Bmem frequency and antigen specificity thus include lengthy ELISA based limiting dilution assays (LDA) requiring 2–3 weeks of stimulation or shorter 3–6 day *in vitro* stimulation methods to convert Bmem into ASC, which are measured by conventional ELISPOT (Slifka and Ahmed, 1996b; Cao et al., 2010; Pinna et al., 2009; Amanna and Slifka, 2006; Jahnmatz et al., 2013; Walsh et al., 2013; Crotty et al., 2004; Buisman et al., 2009). These methods to define Bmem antigen specificity and relative frequencies have focused on peripheral blood or SLT using TLR agonists to stimulate *in vitro* Bmem conversion to ASC. To the best of our knowledge these approaches have not been applied to CNS-derived Bmem which are exposed to a vastly distinct microenvironment. Prolonged isolation procedure of lymphocytes from the CNS as well as their prior *in vivo* exposure to toxic factors may require fine-tuning methods to define Bmem kinetics and specificity during CNS infection, injury, and neurodegeneration.

In the present study, we analyzed Bmem marker expression on CNS infiltrating B cells and optimized *in vitro* stimulation methods to enumerate virus-specific Bmem in the CNS using neurotropic coronavirus JMHV-induced encephalomyelitis. In this model, virus introduced into the brain spreads to spinal cords (Wang et al., 1992). Although T cells clear infectious virus from both organs within 14–16 days post infection (p.i.), virus establishes persistence characterized by low levels of persisting viral RNA and elevated levels of chemokines and cytokines predominantly in spinal cords (Phares et al., 2014). ASC emerging within the CNS after initial viral control maintain persisting viral RNA at low levels and prevent viral recrudescence (Lin et al., 1999; Marques et al., 2011). Isotype-unswitched IgG^- B cells accumulating early during infection are progressively replaced by more differentiated IgD^-IgM^- isotype-switched Bmem and ASC (Phares et al., 2014). ASC are recruited directly to brain and spinal cord in a CXCR3/CXCL10 dependent manner (Marques et al., 2011). Although the initial percentage of ASC within total B cells is similar in brain and spinal cords, ASC accumulate faster and to a higher percentage in spinal cord during viral persistence (Phares et al., 2014). While IgG^+ Bmem emerge in the brain (Phares et al., 2014), their relative recruitment to spinal cords, specificity and potential local conversion to ASC remains unknown. Distinct CD38 and CD73 expression patterns among CNS infiltrating B cells relative to SLT counterparts limited Bmem identification by flow cytometry. Furthermore, *in vitro* Bmem stimulation protocols optimized for splenocytes failed to convert CNS Bmem, suggesting CNS-derived Bmem succumb to cell death. This was supported by reduced pre-existing ASC using similar culture conditions compared to direct *ex vivo* ELISPOT ASC. Comparison of TLR7/8 and TLR9 agonists as Bmem activators, supplementation with feeders and IL-2, as well as reduced culture length revealed optimal CNS-derived Bmem conversion is achieved by 2 day stimulation with the TLR7/8 agonist R848 and irradiated splenocyte feeders. Bmem analysis during JHMV infection indicated Bmem accumulated prominently during chronic infection, similar to ASC, and revealed similar IgG secretion levels as ASC. However, ratios of ASC to Bmem were inverted when comparing brains and spinal cords. Overall, this protocol provides an optimized assay to define Bmem specificity, quantity, and isotype within inflamed CNS tissue.

2. Materials and methods

2.1. Mice and infection

Wild type (WT) C57BL/6 mice were purchased from the National Cancer Institute (Frederick, MD). Six-to seven-week old mice were infected intracranially with 1000 plaque forming units (PFU) of the gliatropic monoclonal Ab derived variant of JHMV designated J.2.2v-1 (Fleming et al., 1986). Cells isolated from brains and spinal cords were used for *in vitro* stimulation and ELISPOT assays. For immunization and splenic B cell analysis, six to seven-week-old mice were injected intraperitoneally (IP) with 1 ml of JHMV DM (9.8×10^6 PFU/ml). All animal procedures were approved by the Institutional Animal Care and Use Committee of the Cleveland Clinic and were conducted in compliance with the Guide for the Care and Use of Laboratory Animals from the National Research Council.

2.2. Tissue dissection and cell isolation

Mice were perfused transcardially with 1 × PBS (Cleveland Clinic Research Institute Cell Services Core, Cleveland, OH) prior to decap-

itation. The skin was removed to expose the skull and a midline incision was made. The skull was then removed to resect the brain. Following brain dissection, the dorsal skin along the spinal column was removed to cut the spinal column at the level of the iliac crest. The spinal cord was flushed at the caudal opening of the spinal column with 1 × PBS using a 10 ml syringe and an 18 gauge needle. Mononuclear cells from spleen, brain, or spinal cord were isolated from pooled organs of 3–4 mice per time point. Spleens were dissociated mechanically and red blood cells lysed. For cell isolation from brains or spinal cords, tissues were minced and digested in 5 ml RPMI 1640 (Cleveland Clinic Research Institute Cell Services Core, Cleveland, OH) supplemented with 10% fetal calf serum (FCS) (Hyclone, Logan, Utah), 100 μl of collagenase type I (100 mg/ml; Worthington Biochemical Corporation, Lakewood, NJ) and 20 μl (200U) of DNAse I (25 mg/ml) (Roche, Indianapolis, IN) for 40 min at 37 °C. Collagenase activity was terminated by addition of 0.1 M EDTA (pH 7.2) at 37 °C for 5 min. Following centrifugation, cells were resuspended in RPMI supplemented with 2% FCS, adjusted to 30% Percoll (GE Healthcare Life Sciences, Pittsburgh, PA) and underlayed with 70% Percoll. After centrifugation for 30 min at 850*g*, mononuclear cells were recovered from the 30/70% Percoll interface and washed with RPMI supplemented with 2% FCS. Cells subjected to flow cytometric analysis were resuspended in fluorescent-activated cell sorter (FACS) buffer (PBS with 0.5% bovine serum albumin), whereas cells for *in vitro* stimulation were resuspended in RPMI 1640 containing 2 mM L-Glutamine, 2 mM non-essential amino acids, 1 mM sodium pyruvate, 25 μg/ml gentamicin, 5×10^{-5} M 2-mercaptoethanol and 10% FCS (RPMI complete).

2.3. Flow cytometric analysis

Cells were incubated in FACS buffer supplemented with 1% mixed serum containing mouse serum (Thermo Fisher Scientific, Waltham, MA), goat serum (Atlanta Biologicals, Flowery Branch, GA), and horse serum (Vector Laboratories, Youngstown, OH) at 1:1:1 and 0.5 μl rat anti-mouse FcγIII/II mAb (2.4G2; BD Bioscience, San Jose, CA) per 10^6 cells for 20 min on ice prior to staining. Expression of cell surface markers was determined by staining on ice for 30 min with Ab specific for CD45 (30-F11; PerCP-Cy5.5), CD19 (1D3; PE-CF594), CD73 (AD2: PE-Cy7) (BD Biosciences, San Jose, CA), IgM (eB131-15F9; PE), IgD (11–26; APC), and CD38 (90; PE) (eBioscience, San Diego, CA). Cells were analyzed on a BD LSRII flow cytometer (BD Biosciences, San Jose, CA) using FlowJo (version 9.7.6) software (Tree Star, Ashland, OR). Doublet exclusion and live gating were applied as previously described (DiSano et al., 2017). Dead cells comprised less than 10% of total SC or brain cells. For all results, plots are representative of 3–4 independent experiments.

2.4. Feeder cells and in vitro stimulation

Splenocytes from naïve C57BL/6 mice were used as feeder layers during B cell stimulation. Following red blood cell lysis and washing, resuspended splenocytes were irradiated with a dose of 3000 rad using a Shepherd irradiator (JL Shepherd and Associates, San Fernando, CA). For stimulation with viral lysate, 60×10^6 splenocytes in 10 ml RPMI complete were mixed with 0.5 ml JHMV lysate (2×10^6 PFU/ml) and incubated for 1 h (h) at 37 °C prior to irradiation. Irradiated feeders with or without viral lysate were washed three times at 450 × g for 5 min and resuspended at 5×10^5 cells in 0.1 ml RPMI complete or RPMI complete containing either 5 μg/ml CpG or 1 μg/ml R848 (InvivoGen, San Diego, CA) and supplemented or not with 10 ng/ml recombinant mouse IL-2 (Biolegend, San Diego, CA). Feeders with various stimulating agents were then plated into 96-well flat-bottom tissue culture plates (Corning, Tewksbury, MA). To block proliferation of stimulated CNS derived effector cells, cell suspensions were also irradiated at 3000 rad, washed, and resuspended in RPMI complete prior to stimulation. Effector cells from CLN, spleens, brains, or spinal cords of JHMV infected WT mice were resuspended at a starting concentration of 1×10 (Pape et al., 2011), 1.25×10 (Taylor et al., 2012), and 1.25×10^4 cells per 0.1 ml RPMI complete containing 5 μg/ml CpG or 1 μg/ml R848 with or without IL-2 10 ng/ml, respectively. Two-fold dilutions (3 wells per dilution; 12 total wells per condition) were plated into 96-well flat-bottom tissue culture plates containing 5×10^5 irradiated feeder splenocytes and incubated for 10 h or 2, 3, 4, or 5 days at 37 °C and 5% CO_2. After stimulation, cells were washed three times with 0.2 ml prewarmed 37 °C RPMI complete per well and centrifuged at 190 × *g* for 5 min. After the last wash, cells were resuspended in 0.2 ml RPMI complete per well and transferred to ELISPOT plates.

2.5. ELISPOT assay

JHMV-specific IgG ASC were measured by ELISPOT assay as previously described (DiSano et al., 2017). Briefly, 96-well PVDF MultiScreen HTS IP plates (EMD Millipore, Billerica, MA) were coated with JHMV DM ($\sim 5 \times 10^5$ PFU/well) overnight at 4 °C. Serial dilutions of cells plated in triplicate were incubated for 4 h at 37 °C and 5% CO_2. ASC was detected by sequential incubation with biotinylated rabbit anti-mouse IgG (0.5 μg/ml; Southern Biotech, Birmingham, AL) overnight at 4 °C, streptavidin horseradish peroxidase (1:1000; BD Biosciences, St. Louis, MO) for 1 h at room temperature, and filtered 3,3′-diaminobenzidine substrate (Sigma-Aldrich, St. Louis, MO) in 0.3% hydrogen peroxide. Brown spots were visible within 2–4 min and the reaction was terminated using cold tap water. Spots were counted using an ImmunoSpot ELISPOT reader (Cellular Technology Ltd., Shaker Heights, OH). Minimum and maximum spot size cutoffs were set to 0.0009 mm^2 and 0.2295 mm^2, respectively and spots were analyzed using diffuse processing and spot separation size of 3.00-5.00. Following automated counting, wells were re-counted manually for exclusion of artifacts. Wells containing ≥4 spots scored positive for virus-specific ASC. For analysis, 3–5 wells within a linear dilution range were averaged for each stimulation condition.

2.6. Statistical analysis

Data were analyzed using Prism (version 6.0) software (GraphPad). Statistical significance between the experimental groups was assessed using a two-tailed paired *t*-test. In all cases, a *P* value of <0.05 was considered significant. Data is representative of 2–3 experiments with 3–4 pooled mice per experiment.

3. Results

3.1. Conventional Bmem markers are expressed on diverse B cell phenotypes within the CNS

Several phenotypic markers have been described to distinguish murine Bmem from mature naïve or other B cell subsets in lymphoid organs, including CD80, PD-L2, CD38 and CD73 (Anderson et al., 2007; Tomayko et al., 2010). However, previous comparative analysis of temporally matched cervical lymph node (CLN) and CNS B cell subsets for expression of the activation marker CD80 and the GC B cell marker GL7 revealed distinct patterns (DiSano et al., 2017). For example, a larger fraction of several CNS B cell phenotypes expressed CD80 compared to peripheral counterparts and expression was sustained, unlike transient expression in CLN. This suggested that conventional phenotypic patterns characterizing B cell subsets, including Bmem, in SLT are insufficient to reliably mark similar subsets in the CNS. We therefore asked if

CD38 and CD73, common markers for murine Bmem within SLT, showed similar expression patterns on B cells derived from CLN *versus* brain during viral encephalomyelitis. The transmembrane receptor CD38 is involved in apoptosis, activation, differentiation, and proliferation (Vences-Catalán and Santos-Argumedo, 2011). CD38 is highly expressed on naïve mature B cells and is downregulated during activation. Its expression is lowest on GC B cells and isotype-switched ASC. By contrast, isotype-switched Bmem exhibit prominent CD38 expression, while expression on GC independent IgM$^+$ Bmem is unclear (Anderson et al., 2007; Ridderstad and Tarlinton, 1998; Vences-Catalán and Santos-Argumedo, 2011). Distinct from CD38, expression of CD73, a surface glycoprotein regulating extracellular ATP and adenosine levels, is low on naïve B cells but upregulated on antigen experienced and GC B cells (Conter et al., 2014). CD73 expression in SLT delineates several subpopulations of Bmem and is absent amongst plasmablasts and plasma cells (Conter et al., 2014; Tomayko et al., 2010).

CD45^{hi} CD19$^+$ B cells from the brain at day 38 p.i. as well as four distinct differentiation subsets defined by their surface Ig as naïve mature B cells (IgD$^+$IgM$^+$), activated B cells (IgD^{int}IgM$^+$), pre-GC/GC/isotype-unswitched (IgD$^-$IgM$^+$) Bmem and isotype-switched Bmem/ASC (IgD$^-$IgM$^-$) were thus compared to analogous CLN day 14 p.i. subsets for CD38 and CD73 expression (Fig. 1). These time points were chosen to reflect abundant B cell subsets in the respective organs. Fig. 1A shows representative gating strategies of the four populations with naïve B cells represented by region 1, activated B cells by region 2 IgD$^-$IgM$^+$ Bmem as region 3 and isotype-switched Bmem/ASC as region 4. Analysis focused on day 14 p.i. when GC formation in CLN is prominent and on day 38 p.i. when more differentiated isotype-switched B cells dominate over less differentiated B cells in the brain during JHMV persistence (Phares et al., 2014; DiSano et al., 2017). Consistent with a minor population of B cells forming GCs and thus a predominant IgD$^+$IgM$^+$ naïve B cell population in CLN throughout infection (Fig. 1A) (DiSano et al., 2017), the vast majority of total CLN B cells (>90%) expressed CD38 at day 14 p.i. (Fig. 1B). While CD38 expression marked all naïve B cells, CD38 progressively decreased on B cells transitioning to an isotype-switched phenotype (Fig. 1B). CD38 expressing cells were reduced to 70% in IgD^{int}IgM$^+$ B cells, to 27% in IgD$^-$IgM$^+$ pre-GC/GC B cells and 13% in IgD$^-$IgM$^-$ isotype-switched cells (Fig. 1B; Populations 1,2,3, and 4, respectively, in Panel A), which comprise a relatively small proportion of CD19$^+$ cells within the CLN (DiSano et al., 2017). Brain CD19$^+$ B cells revealed overall reduced CD38 expression (65%) compared to the CLN (Fig. 1C). While IgD$^+$IgM$^+$ B cells also all expressed CD38 (99%), a smaller proportion of more differentiated cells downregulated CD38 compared to their CLN counterparts. Although expression was progressively lower relative to the naïve population in activated (IgD^{int}IgM$^+$), pre-GC/isotype-unswitched Bmem (IgD$^-$IgM$^+$), and isotype-switched B cells (IgD$^-$IgM$^-$), the percentage of CD38$^+$ cells remained >50% even in the isotype-switched population (Fig. 1C).

The pattern of CD73 expression was even more diverse than CD38 between B cell subsets in CLN and brain (Fig. 1D and E). In CLN, the proportion of CD73$^+$ cells in total CD19B cell was <10%, coincident with sparse expression in naïve IgD$^+$IgM$^+$ B cells. Expression remained low on IgD^{int}IgM$^+$ B cells (~10%; Fig. 1D), but was increased on IgD$^-$IgM$^+$ cells (41%). The proportion of CD73$^+$ cells was the highest (80%) in isotype-switched IgD$^-$IgM$^-$ B cells. This profile is consistent with CD73 upregulation on antigen experienced and GC B cells (Conter et al., 2014). Relative to CLN, CD73 expression was 4-fold higher (41%) among CNS infiltrating CD19$^+$ B cells, reflecting higher proportions of activated and isotype-switched B cells accumulating in the CNS during persistence. However, with the exception of naïve B cells, CD73 was differently regulated on the corresponding B cell subpopulations within the brain (Fig. 1E). IgD^{int}IgM$^+$ B cells segregated into a population of no or low expressors and ~50% CD73 high expressors. The IgD$^-$IgM$^+$ B cells were also split into a CD73 non-expressing and expressing phenotype, although CD73 expression levels were slightly lower than in IgD^{int}IgM$^+$ B cells. Isotype-switched IgD$^-$IgM$^-$ B cells exhibited an even more pronounced decline in both the proportion and intensity of CD73 expression (Fig. 1E). Whether the distinct patterns of CD38 and CD73 expression on CNS *versus* CLN B cells reflects preferential recruitment or local influences remains unclear. Nevertheless, the data clearly indicate that activation or Bmem markers characterizing B cell subsets in lymphoid tissue are not suitable to identify CNS B cell subsets.

3.2. Bmem LDA optimized for SLT leads to minimal CNS bmem conversion

Culture conditions designed to quantify virus-specific Bmem have largely been optimized using cells derived from lymphoid tissue and rely on various *in vitro* stimulation strategies to convert Bmem into ASC, which are then measured by ELISPOT in a separate plate. *In vitro* this process requires proliferation and thus prolonged stimulation more than 24 h, the minimum time required to trigger division by Bmem (Slifka and Ahmed, 1996b). For instance, following LCMV infection maximal virus-specific Bmem conversion into ASC was initially achieved by stimulating splenocytes from LCMV infected mice at serial dilutions with irradiated LCMV infected carrier splenocytes as a source of viral antigen for 6 days p.i (Slifka and Ahmed, 1996b). Although *in vitro* stimulation often relies on nonspecific polyclonal activators as infected cells often provide insufficient antigen stimulus, specific antigen stimulation is more selective as it minimizes excessive B cell proliferation and bystander Ab production to irrelevant antigens (Hebeis et al., 2004). To apply virus-specific *in vitro* stimulation LDA to JHMV infection, we initially infected mice IP, harvested splenocytes at day 28 p.i. and stimulated serial cell dilutions in 96-well flat bottom culture plates with irradiated feeders pre-incubated with viral lysate for 4, 5, or 6 days at 37 °C. After *in vitro* stimulation, and washing to remove virus and antibody, cells were transferred to virus-coated ELISPOT membrane plates and incubated at 37 °C for 4 h to detect virus-specific IgG ASC. ASC quantified after stimulation reflect both pre-existing ASC and ASC derived from Bmem. To quantify pre-existing ASC, serial splenocyte dilutions were subjected to a direct *ex vivo* 4 h ELISPOT assay. Decreased ASC frequencies following incubation with viral lysate for 4 or 6 days relative to 5 days (data not shown), revealed 5 days stimulation was optimal for ASC survival and Bmem conversion following peripheral JHMV infection. However, splenocyte stimulation with feeders pre-incubated with viral lysate alone did not increase ASC frequencies relative to *ex vivo* ELISPOT analysis (Fig. 2A). These results suggested viral lysate provided insufficient stimulation to mediate Bmem conversion.

Bmem proliferation and conversion to ASC can be stimulated using pokeweed mitogen (PWM) or TLR agonists, including synthetic oligonucleotide CpG (TLR9 agonist) and R848 (TLR7/8 agonist), which selectively convert Bmem, but not naïve B cells into ASC (Cao et al., 2010; Pinna et al., 2009; Jahnmatz et al., 2013; Walsh et al., 2013; Crotty et al., 2004; Hawkins et al., 2013). We therefore initially used CpG as a common polyclonal activator to specifically enhance conversion of splenic Bmem and not naïve B cells from JHMV immune mice. CpG was added to either irradiated feeders alone or feeders pre-incubated with viral lysate to stimulate JHMV Bmem for 4, 5, or 6 days as described above. ELISPOT analysis revealed 5 days stimulation was superior to 4 or 6 days in achieving highest ASC frequencies (data not shown). Furthermore, optimal CpG mediated Bmem to ASC conversion was independent of viral lysate (Fig. 2A). Virus-specific IgG ASC frequencies were 2-fold higher (~300) following stimulation compared to direct *ex vivo* ELISPOT analysis (~150). Lastly, splenocyte CpG stimulation

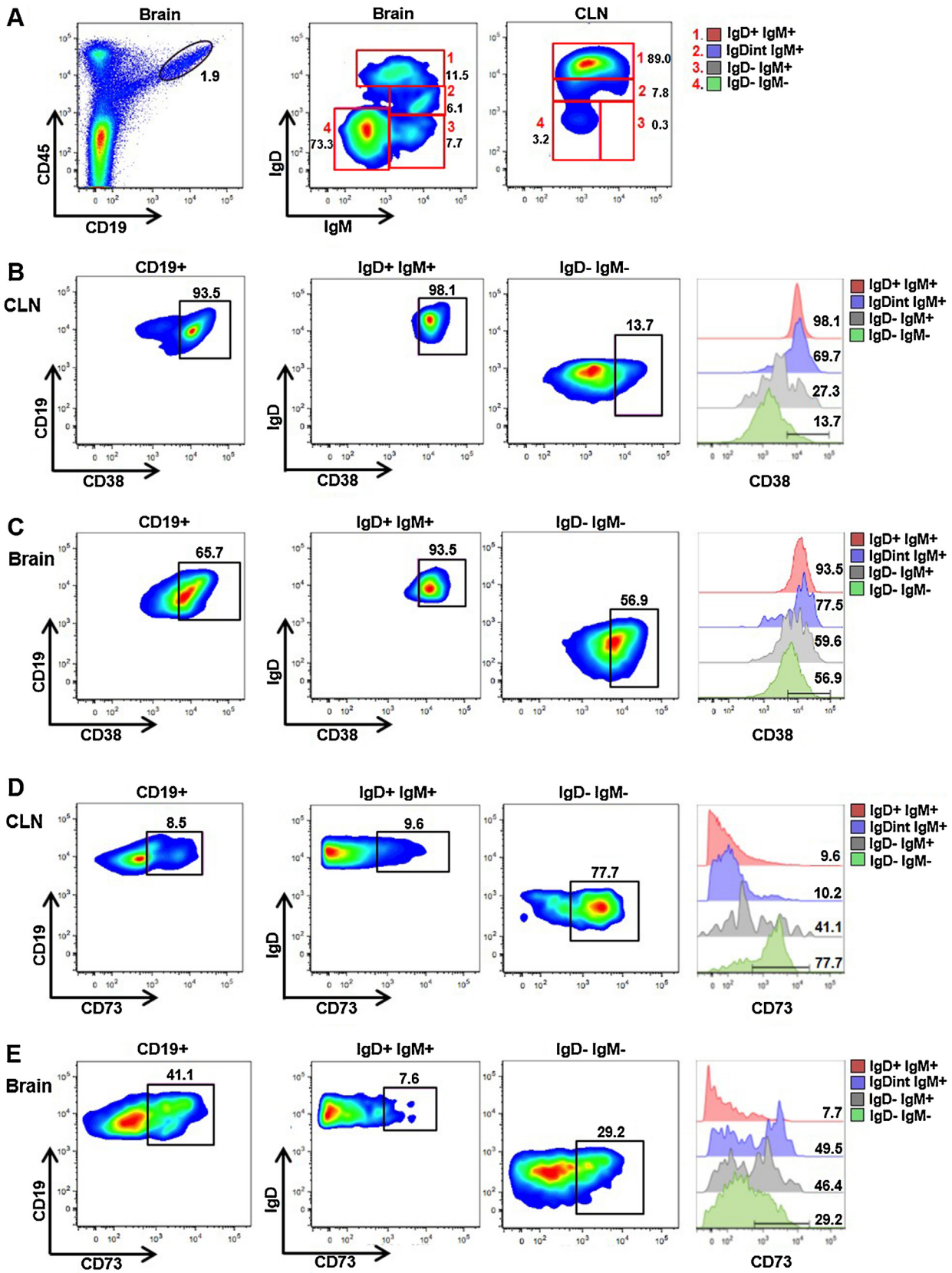

Fig. 1. Bmem markers on CNS infiltrating B cells have distinct surface expression from the periphery. Brain and CLN cells isolated from pooled organs of JHMV infected mice at day 14 (CLN) and day 38 (brain) p.i. were analyzed for CD38 and CD73 expression. (A) Representative gating strategy for $CD19^+$ infiltrating B cells in the brain and gating of IgD^+ and IgM^+ subsets in the brain and CLN. Representative density plots depict CD38 (B-C) and CD73 (D-E) expression among total $CD19^+$, naïve IgD^+IgM^+, and IgD^-IgM^- isotype switched B cells within the CLN (B, D) and brain (C, E). Representative histograms depict CD38 or CD73 expression among naïve IgD^+IgM^+, activated $IgD^{int}IgM^+$, IgD^-IgM^+, and isotype-switched ASC/Bmem IgD^-IgM^- B cells within the CLN and brain. Data is representative of 3–4 independent experiments.

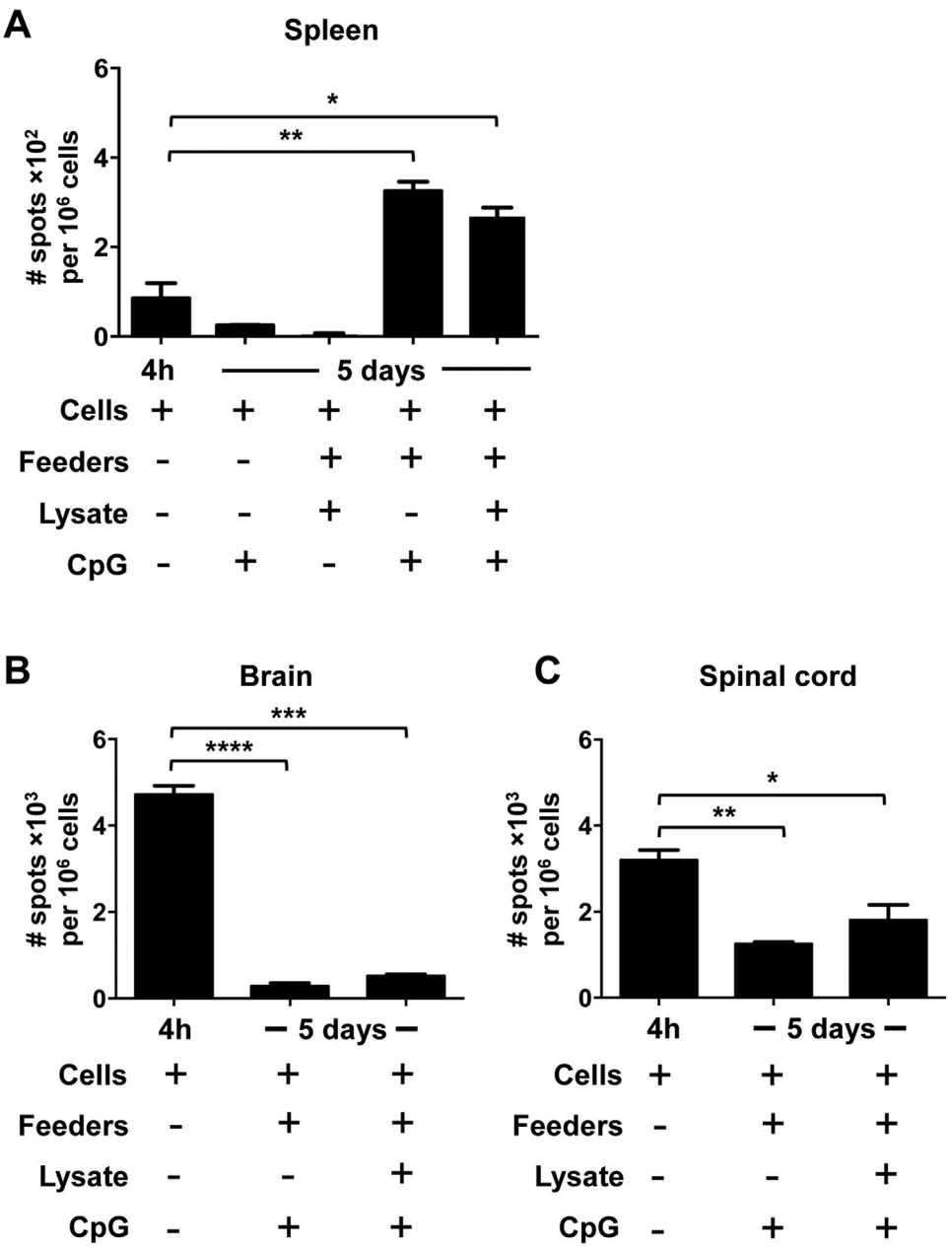

Fig. 2. Stimulation conditions optimized for spleen Bmem conversion results in minimal conversion/survival for CNS isolated B cells. Cells isolated from spleen (A), brain (B), or spinal cord (C) of infected mice at day 28 p.i. were stimulated for 5 days under various conditions including: 1) CpG, 2) irradiated feeders pre-incubated with viral lysate, 3) CpG with irradiated feeders, or 4) CpG with irradiated feeders pre-incubated with viral lysate. After culture, virus-specific IgG secreting ASC were enumerated by ELISPOT using virus coated plates. Pre-existing ASC numbers were determined by 4 h (h) direct *ex vivo* ELISPOT. Data represents the mean ± SEM ASC per 10^6 cells based on cells plated prior to CpG stimulation from 3 to 4 pooled mice. ASC frequencies per animal were determined using the average frequencies of 3–5 wells showing spots within linear dilution range. Data are representative of 2 independent experiments. Significant differences between conditions at 4 h and 5 days indicated by * $p \leq 0.05$, ** $p \leq 0.01$, *** $p \leq 0.001$, and **** $p \leq 0.0001$.

for 5 days in the absence of feeders decreased ASC recovery compared to direct *ex vivo* ELISPOT analysis suggesting feeders provide survival factors.

The same *in vitro* stimulation method used for JHMV immune splenocytes was applied to analyze virus-specific IgG Bmem in brain and spinal cord following intracranial JHMV infection. Moreover, surface IgG^+ $CD138^-$ B cells indicative of Bmem are detectable at day 28 p.i. during persisting JHMV infection (Phares et al., 2014). To examine Bmem specificity, single cell suspensions from brains and spinal cords at day 28 p.i. were serially diluted and stimulated under optimal conditions previously determined for splenic B cells using CpG for 5 days in the presence of irradiated feeders with or without viral lysate. Cells were then transferred to ELISPOT plates and assessed for virus-specific IgG ASC (Fig. 2B). We focused on IgG as the vast majority (~70%) of isotype switched virus specific ASC in the CNS secrete IgG isotype Ab, with a minor contribution of IgA secreting ASC (Tschen et al., 2002). Pre-existing virus-specific ASC were measured in a direct 4 h *ex vivo* ELISPOT assay. In contrast to splenocytes, neither brain or spinal cord cells revealed Bmem to ASC conversion, as indicated by no increase in spots relative to the numbers obtained from direct *ex vivo* ELISPOT analysis. This finding was independent of addition of viral lysate. Rather than increasing, virus-specific ASC after CpG stimulation were actually 3-fold lower in the brain (~1×10^3 ASC) and 2-fold lower in the SC

($\sim 2 \times 10^3$ ASC) relative to pre-existing ASC (Fig. 2B,C). This suggested that cell death during strong stimulation and prolonged culture of CNS cells or loss in the washing/transfer procedure leads to premature attrition of pre-existing ASC. This is supported by studies with LCMV, which have suggested direct *ex vivo* ASC assays may yield higher ASC frequencies than those observed after prolonged culture, thereby complicating calculations and potentially underestimating ASC converted from Bmem (Slifka and Ahmed, 1996b).

3.3. In vitro *stimulation reduces pre-existing ASC from the CNS*

The discrepancy in Bmem conversion after stimulation in the spleen *versus* CNS implied that while the CNS environment can sustain Bmem or ASC survival, survival is limited when explanted. We therefore assessed how distinct *in vitro* stimulation conditions including the TLR agonists CpG (TLR9) and R848 (TLR7/8) affect CNS derived pre-existing virus-specific IgG ASC. To minimize cell death due to prolonged culture, incubation was limited to 2 days, which increased ASC frequencies compared to 4 or 5 days stimulation in initial studies (data not shown). Pre-existing ASC were measured in serial dilutions of CNS-derived cells at day 28 p.i. using four conditions: a) direct *ex vivo* 4 h ELISPOT, b) stimulation with R848 or CpG for 10 h, which is insufficient time for Bmem to differentiate into ASC (Slifka and Ahmed, 1996b), c) stimulation with R848 or CpG supplemented with feeders for 2 days, but irradiation of CNS cells to block cellular division (Slifka and Ahmed, 1996b) and lastly d) culture with splenocyte feeder cells only for 2 days to assess whether feeder-derived supplements sustain pre-existing ASC. Following the distinct culture conditions, serially diluted cells were transferred to ELISPOT membranes and assessed for virus-specific IgG ASC 4 h later. ASC obtained from *in vitro* stimulation controls were compared to pre-existing ASC obtained by direct *ex vivo* ELISPOT (Fig. 3). Fig. 3 only includes data from R848 stimulation as CpG and R848 stimulation produced interchangeable results (data not shown). 10 h culture with R848 already reduced ASC frequencies relative to *ex vivo* ASC numbers to ~30% in both brain and spinal cord-derived cells. However, 2 day stimulation conditions did not further reduce pre-existing ASC numbers. All culture conditions yielded $\sim 1 \times 10^3$ pre-existing ASC within the brain and $\sim 5 \times 10^3$ within the spinal cord, which represents a ~3-fold reduction compared to direct ASC assays. These consistent control results suggested multiple wash steps and transfer to ELISPOT membranes reduce ASC recovery ~3-fold. Importantly, the differing *in vitro* controls abrogating Bmem conversion all resulted in similar virus-specific IgG ASC, demonstrating reproducible calculation of pre-existing ASC. Exposure of pre-existing ASC to the same culture conditions as Bmem thus underestimates ASC but provides a more valid approach to assess ASC derived from Bmem conversion relative to pre-existing ASC, than comparison to ASC numbers obtained from direct *ex vivo* ELISPOT.

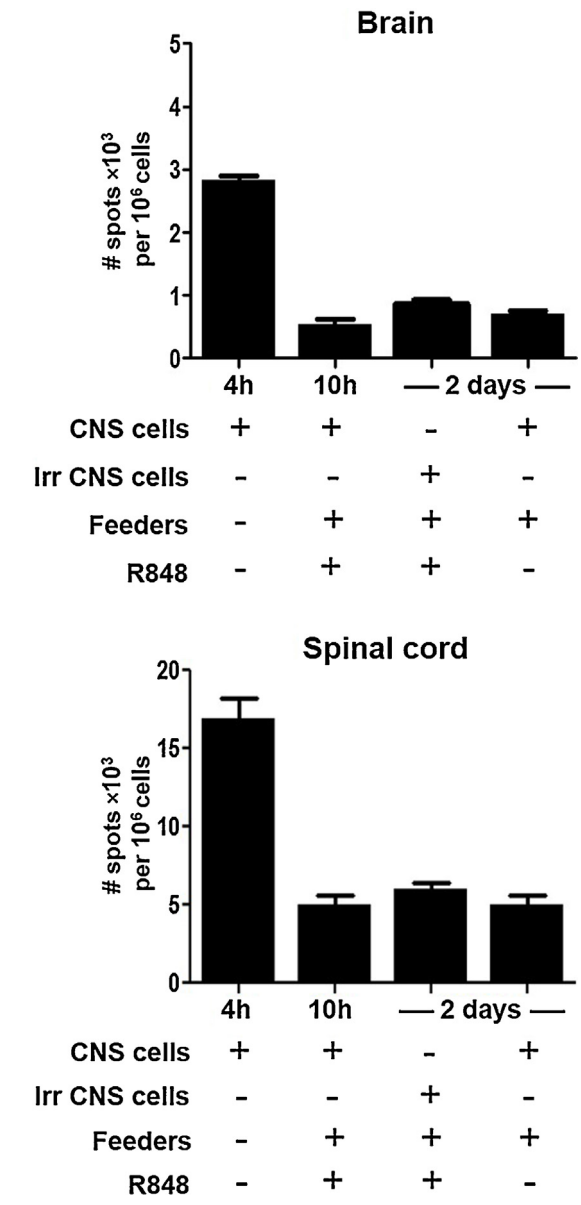

Fig. 3. *in vitro* stimulation protocol reduces ASC numbers. Cells isolated from brain or spinal cord of infected mice at day 38 p.i. were stimulated for 10 h or 2 days with R848 in the presence of irradiated splenocyte feeders as indicated. Direct *ex vivo* ASC quantification was conducted using 4 h incubation on ELISPOT plates. For 10 h ASC controls, CNS cells were cultured with splenoctye feeders with R848 stimulation. For 2 day (d) ASC controls, splenocyte feeders were cultured with irradiated CNS cells with R848 stimulation or CNS cells without stimulation. After culture, virus-specific IgG secreting ASC were enumerated by ELISPOT using virus coated plates. Data represents the mean + SEM ASC per 10^6 cells prior to stimulation from 3 to 4 pooled mice. ASC frequencies per animal were determined using the average frequencies of 3–5 wells showing spots within linear dilution range. Data are representative of 1–2 independent experiments.

3.4. *Optimizing CNS bmem conversion*

To optimize CNS derived Bmem conversion, we next examined the effects of TLR agonists R848 and CpG under various culture conditions using CNS cells from persistently infected mice at days 28–38 p.i. R848 stimulation of human PBMCs and murine splenocytes has been recently shown to enhance Bmem conversion compared to CpG stimulation, suggesting R848 may be a superior stimulating agent (Jahnmatz et al., 2013). Bmem conversion was evaluated relative to pre-existing ASC numbers obtained from irradiated CNS cells stimulated for 2 days under the same conditions (Fig. 4A). As expected, feeder cells themselves showed no detectable ASC even when cultured with TLR agonists (Fig. 4A). Coculture of brain-derived cells with feeders alone improved recovery of virus-specific ASC, relative to no feeders, supporting feeders provide survival factors. However, feeders did not significantly enhance ASC frequencies in spinal cord-derived B cells (Fig. 4A), suggesting they may be less prone to death than brain counterparts. CpG stimulation resulted in a modest increase of virus-specific ASC in brain derived, but not spinal cord-derived cells compared to feeders alone. By contrast, R848 stimulation significantly increased virus-specific ASC by 2–3-fold relative to pre-existing ASC in both brain and spinal cord cells. Irradiation of CNS effector cells reduced CpG and R848 ASC frequencies back to feeder only culture fre-

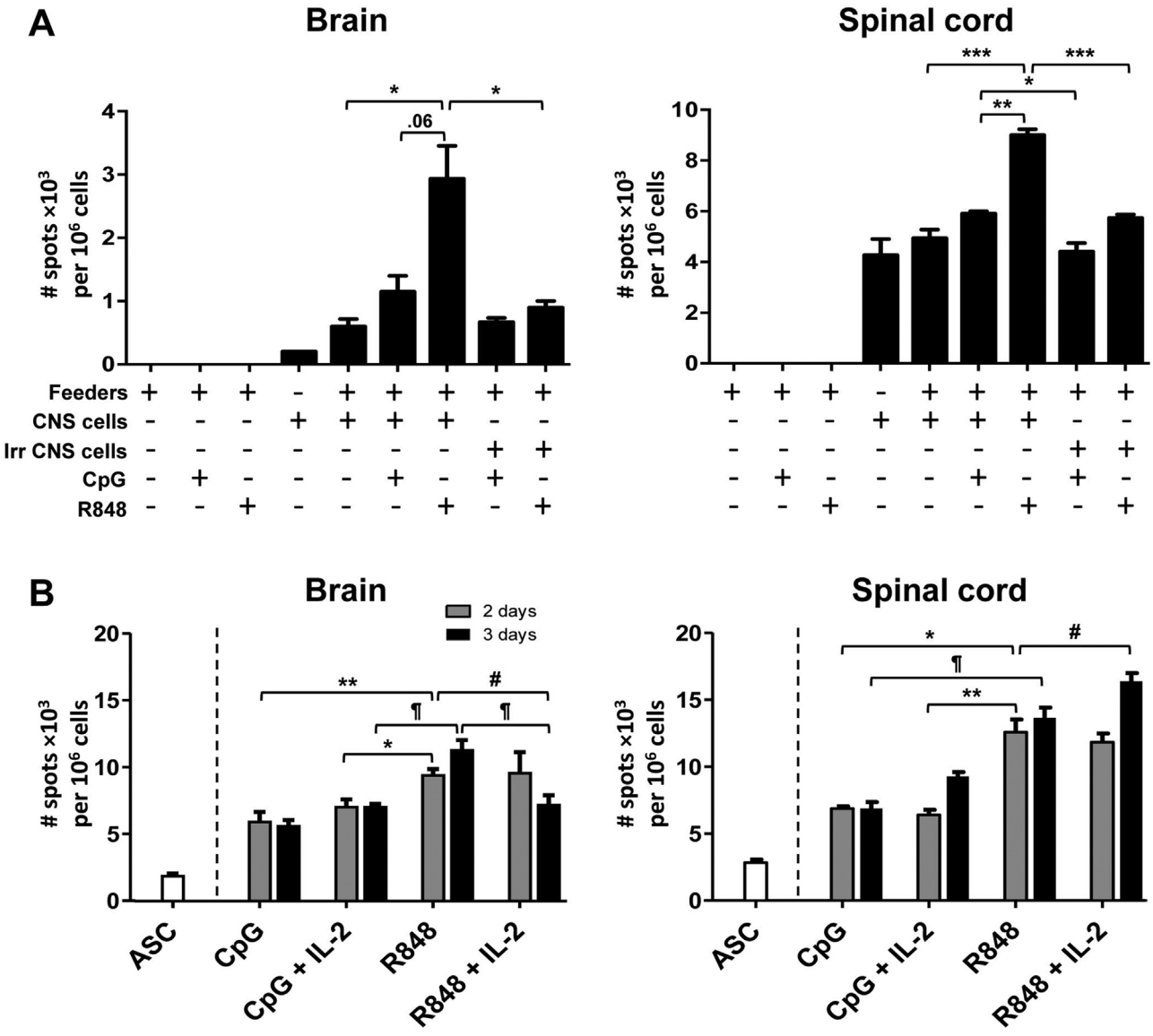

Fig. 4. 2 day R848 stimulation provides optimal ASC conversion for CNS-derived Bmem. (A) Cells isolated from brain or spinal cord of infected mice at day 38 p.i. were incubated with irradiated feeders plus R848 or CpG for 2 days as indicated. (B) Cells isolated from brain or spinal cord of infected mice at day 28 p.i. were stimulated with CpG or R848 with or without IL-2 in the presence of irradiated splenocyte feeders for 2 or 3 days. After culture, virus-specific IgG secreting ASC were enumerated by ELISPOT using virus coated plates. Data represents the mean + SEM ASC per 10^6 cells based on cells plated prior to stimulation from 3 to 4 pooled mice. ASC frequencies per animal were determined using the average frequencies of 3–5 wells showing spots within linear dilution range. Data are representative of 2 independent experiments. Significant differences between conditions in panel A indicated by * $p \leq 0.05$, ** $p \leq 0.01$, *** $p \leq 0.001$. In panel B significant differences comparing conditions either at day 2 or day 3 indicated by * $p \leq 0.05$, ** $p \leq 0.01$, and ¶ $p \leq 0.05$, respectively; significant differences comparing conditions between days 2 and 3 indicated by # $p \leq 0.05$.

quencies (Fig. 4A). These results confirmed that increased ASC frequencies following TLR stimulation indeed resulted from Bmem proliferation and conversion. Importantly, as Bmem proliferation is only initiated after 24 h, the 2 day stimulation period limits proliferation to 1–2 divisions thereby minimizing artificially high Bmem frequencies due to numerous divisions (Slifka and Ahmed, 1996b; Tangye and Hodgkin, 2004; Bernasconi et al., 2002).

Supplementation of media with IL-2 either using ConA conditioned medium or recombinant IL-2 has been shown to enhance cell survival and Bmem conversion in *in vitro* Bmem stimulation assays (Slifka and Ahmed, 1996b; Walsh et al., 2013). To test whether CNS Bmem conversion could be further increased, we expanded stimulation times to 3 days and supplemented media with IL-2. However, neither increased culture duration nor addition of IL-2 to CpG stimulation enhanced Bmem to ASC conversion in brain derived cells, independent of stimulation for 2 or 3 days (Fig. 4B). Furthermore, IL-2 only improved ASC recovery after 3 day, but not 2 day culture in CpG stimulated spinal cord cells. While prolonged culture time modestly increased brain derived virus-specific ASC following R848 stimulation, IL-2 addition had no enhancing effects. Prolonged stimulation also had no beneficial effects on Bmem conversion in R848 stimulated spinal cord cells and IL-2 only modestly increased ASC after 3 days stimulation. Overall, these results confirmed superior stimulation by R848 compared to CpG, independent of prolonged culture or IL-2 addition. We therefore chose R848 stimulation for 2 days as optimal for Bmem conversion in CNS derived cells.

3.5. ASC:Bmem ratios during JHMV infection

JHMV infection induces virus-specific IgG ASC expansion within the draining cervical lymph nodes (CLN) at day 14 p.i coincident

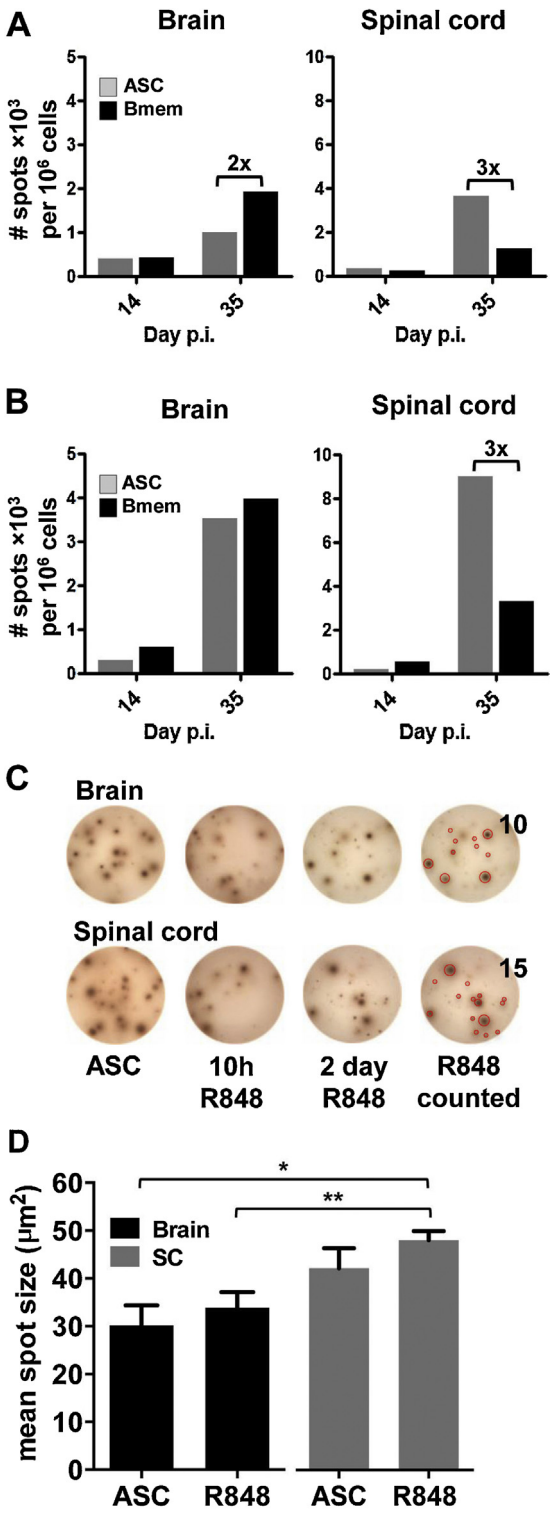

Fig. 5. Bmem emerge with similar kinetics to ASC in the CNS. (A-B) Cells isolated from brain or spinal cord of infected mice at day 14 and 35 p.i. CNS cells were stimulated with R848 in the presence of irradiated splenocytes. After culture, virus-specific IgG secreting ASC were enumerated by ELISPOT using virus coated plates. Pre-existing ASC numbers are calculated from R848 stimulated irradiated CNS cells incubated with splenocyte feeders. Bmem numbers are calculated based on total ASC numbers after R848 stimulation minus pre-existing ASC numbers. Data represents the mean ± SEM ASC per 10^6 cells based on cells plated prior to nonspecific stimulation from 3 to 4 pooled mice. Mean values are calculated from 5 wells showing spots within the linear dilution range. Two independent experiments revealed similar ASC/Bmem kinetics throughout infection. (C) Spot size of brain or spinal cord-derived ASC following direct *ex vivo* 4 h incubation (ASC) and 10 h or 2 day R848 stimulation. R848 counted highlights ASC counted for 2 day R848 stimulation well. (D) Mean ± SEM ASC spot size following direct *ex vivo* ELISPOT (ASC) and ASC after 2 day R848 stimulation (R848) in the brain and spinal cord (SC). Data are representative of 2–3 independent experiments. Significant differences between brain and spinal cord indicated by * $p \leq 0.05$, and ** $p \leq 0.01$.

with GC formation (DiSano et al., 2017; Tschen et al., 2002). Virus-specific IgG initially accumulates in the brain and spinal cord, but preferentially increases in the spinal cord, the site of viral persistence and low, but ongoing inflammation (Phares et al., 2014). Increased virus specific IgG in spinal cords by day 21 p.i. correlates with the overall increased fraction of ASC compared to the brain (Phares et al., 2014; Phares et al., 2016). Using the assay conditions optimized above, we assessed Bmem numbers relative to ASC in the CNS during JHMV infection at the onset of ASC emergence at day 14 and during persistence at day 35 p.i. (Tschen et al., 2002). Reproducibility and kinetics of virus-specific IgG Bmem and pre-existing ASC was evaluated in the brain and spinal cord in independent experiments (Fig. 5A, B), as biological variability in immune responses to infection and efficiency in CNS cell isolation can lead to differences in absolute frequencies between multiple experiments. Pre-existing ASC were calculated using the average of 4–5 wells in a linear dilution range from irradiated CNS cells cultured with R848 and feeders. Virus-specific IgG Bmem were calculated by subtracting the average pre-existing ASC from the average number of ASC obtained after R848 stimulation. Virus-specific ASC progressively accumulated within the CNS during persistence, with elevated frequencies in spinal cord at day 35 p.i., confirming previous results (Phares et al., 2014; Tschen et al., 2002). Virus-specific Bmem frequencies in the brain were comparable to ASC at day 14 p.i. (~500 cells), and increased between 5–8-fold by day 35 p.i. (Fig. 5A, B). Furthermore, Bmem surpassed ASC frequencies in the brain by 1.2–2-fold by day 35 p.i. Spinal cords also revealed similarly low frequencies of Bmem and ASC at day 14 p.i., with both increasing by day 35 p.i. Although the increase relative to day 14 p.i. ranged between 3–5-fold, virus-specific ASC frequencies were overall 3-fold higher than Bmem. While the ratio of ASC to Bmem was ~0.7 in the brain, it was inverted at 3.0 in spinal cord when averaging results from 2 separate experiments. Furthermore, in contrast to preferential accumulation of ASC in the spinal cord during chronic infection, Bmem were similar within the brain and spinal cord at day 35 p.i. It remains unclear whether the site of enhanced viral persistence preferentially affects ASC over Bmem accumulation, or whether the spinal cord environment can mediate local conversion of Bmem to ASC.

Detection of virus-specific Bmem in the CNS led us to examine Bmem derived ASC IgG secretion capacity compared to pre-existing ASC. Spot diameter and intensity reflect both Ig secretion rates and affinity, with large and intense spots indicative of more differentiated, high affinity ASC (Sibley et al., 2012; Thomson, 2005; Feske et al., 2012; Karulin and Lehmann, 2011). Therefore, we investigated Ig secretion by quantifying spot size of virus-specific IgG derived from converted ASC after 2 days R848 stimulation *versus* pre-existing ASC from direct *ex vivo* ELISPOT (Henn et al., 2009). As an additional control, ASC spot size after 10 h R848 stimulation was compared to control for effects of *in vitro* stimulation on pre-existing ASC spot size (Fig. 5C). Quantification revealed no significant difference in ASC spot size after 10 h stimulation *versus* direct *ex vivo* ELISPOT (data not shown). More importantly, virus-specific IgG spot size from brain derived ASC measured directly by *ex vivo* ELISPOT assays and those ASC formed 2 days post R848 stimulation was also similar at a mean spot size of 30–40 μm^2 (Fig. 5C, D). Similarly, spot size analysis of spinal cord-derived cells revealed no significant difference between ASC after R848 stimulation compared to direct *ex vivo* ELISPOT. Nevertheless, the mean spot size was 40–50 μm^2, suggesting enhanced IgG secretion for ASC and

Bmem in the spinal cord relative to brain (Fig. 5C, D). The *in vitro* stimulation assay established for CNS derived Bmem is therefore a useful tool to quantify and determine Bmem specificity and can be adapted to assess isotype variants and Ig secretion levels during heterologous CNS inflammation models.

4. Discussion

The presence of B cells with multiple differentiation phenotypes in the CNS following various insults, including infection, has reinvigorated research into mechanisms supporting their accumulation, function, and specificity. The recruitment of ASC into the CNS and their specificity following viral encephalomyelitis is well documented in animal models (Tschen et al., 2002; Metcalf et al., 2013). ASC have also been detected in the CSF of patients afflicted by viral encephalitis and multiple sclerosis (Krumbholz et al., 2012; Burke et al., 1985; Jacobi et al., 2007; Kapoor et al., 2004; Linnoila et al., 2016; Skoldenberg et al., 1981). However, the presence of Bmem and their specificity has not been studied extensively due to methodological limitations in determining specificity. As Bmem require minimal stimulation to convert to ASC compared to naïve B cells (Kurosaki et al., 2015), they are ideal candidates to locally differentiate and sustain Ab responses. Persisting antigen, T helper cells, cytokines, and TLR agonists all present in the inflamed CNS have the potential to induce Bmem differentiation into ASC (Kurosaki et al., 2015; Hebeis et al., 2004; Aiba et al., 2010; Geffroy-Luseau et al., 2011). During viral encephalitis, antigen specific Bmem may locally contribute to humoral responses and serve a protective role in controlling infectious virus. However, Bmem directed against self-antigens during neurodegeneration, autoimmunity, or injury, may enhance pathogenic responses.

JHMV induced acute encephalomyelitis resolving into persistence has provided an excellent model to study progression and maintenance of humoral responses within the CNS. The accumulation of isotype-switched IgG^+ $CD138^-$ $CD19^+$ B cells, characteristic of Bmem, in both the brain and spinal cord during persistent infection led us to assess their specificity using established Bmem to ASC conversion protocols developed for B cells in lymphoid organs. However, several unsuccessful trials to apply these procedures to CNS B cells prompted us to tailor culture conditions to enhance Bmem to ASC conversion as well pre-existing ASC survival.

To yield high numbers of viable CNS cells which retain all classical B cell surface markers, the protocol uses collagenase-based digestion of CNS tissue. The initial LDA *in vitro* culture conditions mainly differ from other LDA stimulation protocols by utilizing shorter R848 mediated TLR7/8 stimulation periods to circumvent B cell loss presumably due to cell death. Moreover, addition of irradiated feeder cells improved survival of ASC/Bmem, while IL-2 supplementation has no beneficial effect. Although the shortened 2 day stimulation period minimized cell death, significant cell loss in the wash and transfer process was evident by a similar reduction in pre-existing ASC after both 10 h and 2 day stimulation compared to direct *ex vivo* ELISPOT. Although *ex vivo* stimulation directly on ELISPOT membranes thus appears ideal to minimize cell loss, prolonged incubation of cells on ELISPOT membranes leads to increased background, artefacts due to cell debris, and increased spot density due to high levels of Ab secretion. An obvious caveat of the *in vitro* stimulation on 96 well flat bottom culture plates is thus that Bmem and ASC frequencies may be underestimated by 3-fold as indicated by our control experiments with pre-existing ASC. *In vitro* stimulation controls inhibiting Bmem conversion are thus necessary to standardize cell loss and compare the ratio of Bmem to pre-existing ASC.

Another caveat of Bmem stimulation prior to ELISPOT analysis is the use of polyclonal stimulators such as TLR agonists, which induce rapid proliferation regardless of antigen specificity, thereby potentially overestimating Bmem numbers based on ASC conversion. *In vitro* stimulation utilizing feeders presenting virus antigen would limit non-specific, rapid proliferation resulting in a more accurate assessment of virus-specific Bmem. However, incubation of virus lysate with feeders was insufficient to convert Bmem in our system presumably due to limiting virus dose. Nevertheless, fairly short stimulation times of 2 days in addition to use of virus coated ELISPOT plates limit proliferation and the potential for skewed virus-specific IgG ASC within total IgG ASC. Although future studies aim to optimize stimulation using feeders incubated with distinct viral antigens to induce more physiologically relevant Bmem conversion, a caveat in the JHMV system is that spike protein binds to CEACAM1, which is highly expressed on B cells and itself a signaling molecule (Williams et al., 1990; Greicius et al., 2003; Khairnar et al., 2015).

In summary, our optimized LDA *in vitro* stimulation ELISPOT assay provides a tool for simultaneous analysis of CNS derived Bmem and ASC during neuroinflammatory diseases, including microbial infection, autoimmunity, or tissue injury. The relatively short 2.5–3 day combined *in vitro* stimulation LDA/ELISPOT procedure is more efficient than previously described 2–4 week stimulation ELISA based Bmem assays, which measure secreted Ab. The assay allows for assessment of Bmem antigen specificity, isotype and kinetic alterations throughout disease, and are complementary to enumerating Bmem based on surface marker profiles. Comparative assessment of Bmem in SLT and the CNS will aid in understanding the relationship between peripheral Bmem and CNS accumulation during disease and identifying tissue specific therapeutics to either enhance or diminish Bmem during neuroinflammatory diseases.

Acknowledgements

This work was supported by US National Institutes of Health grant NS086299. The funding source had no involvement in the study design, writing of the manuscript, decision to submit, or collection, analysis, and interpretation of data. We sincerely thank Mi Widness and Dr. Alice Valentin-Torres for preparation of splenocyte feeder cells and Mi-Hyun Hwang for viral CNS infection.

References

Adlowitz, D.G., et al., 2015. Expansion of activated peripheral blood memory b cells in rheumatoid arthritis, impact of B cell depletion therapy, and biomarkers of response. PLoS One 10, e0128269.

Aiba, Y., et al., 2010. Preferential localization of IgG memory B cells adjacent to contracted germinal centers. Proc. Natl. Acad. Sci. U. S. A. 107, 12192–12197.

Amanna, I.J., Slifka, M.K., 2006. Quantitation of rare memory B cell populations by two independent and complementary approaches. J. Immunol. Methods 317, 175–185.

Amu, S., Tarkowski, A., Dörner, T., Bokarewa, M., Brisslert, M., 2007. The human immunomodulatory CD25+ B cell population belongs to the memory B cell pool. Scand. J. Immunol. 66, 77–86.

Anderson, S.M., Tomayko, M.M., Ahuja, A., Haberman, A.M., Shlomchik, M.J., 2007. New markers for murine memory B cells that define mutated and unmutated subsets. J. Exp. Med. 204, 2103–2114.

Ankeny, D.P., Guan, Z., Popovich, P.G., 2009. B cells produce pathogenic antibodies and impair recovery after spinal cord injury in mice. J. Clin. Invest. 199, 2990–2999.

Bernasconi, N.L., Traggiai, E., Lanzavecchia, A., 2002. Maintenance of serological memory by polyclonal activation of human memory B cells. Science 298, 2199–2202.

Buisman, A.M., de Rond, C.G., Oztürk, K., Ten Hulscher, H.I., van Binnendijk, R.S., 2009. Long-term presence of memory B-cells specific for different vaccine components. Vaccine 28, 179–186.

Burke, D.S., Nisalak, A., Lorsomrudee, W., Ussery, M.A., Laorpongse, T., 1985. Virus-specific antibody-producing cells in blood and cerebrospinal fluid in acute Japanese encephalitis. J. Med. Virol. 17, 283–292.

Cao, Y., et al., 2010. An optimized assay for the enumeration of antigen-specific memory B cells in different compartments of the human body. J. Immunol. Methods 358, 56–65.

Cepok, S., et al., 2006. Accumulation of class switched IgD-IgM- memory B cells in the cerebrospinal fluid during neuroinflammation. J. Neuroimmunol. 180, 33–39.
Conter, L.J., Song, E., Shlomchik, M.J., Tomayko, M.M., 2014. CD73 expression is dynamically regulated in the germinal center and bone marrow plasma cells are diminished in its absence. PLoS One 9, e92009.
Crotty, S., Aubert, R.D., Glidewell, J., Ahmed, R., 2004. Tracking human antigen-specific memory B cells: a sensitive and generalized ELISPOT system. J. Immunol. Methods 286, 111–122.
Dang, A.K., Tesfagiorgis, Y., Jain, R.W., Craig, H.C., Kerfoot, S.M., 2015. Meningeal infiltration of the spinal cord by non-classically activated b cells is associated with chronic disease course in a spontaneous B cell-dependent model of CNS autoimmune disease. Front. Immunol. 6, 470.
DiSano, K.D., Stohlman, S.A., Bergmann, C.C., 2017. Activated GL7(+) B cells are maintained within the inflamed CNS in the absence of follicle formation during viral encephalomyelitis. Brain Behav. Immun. 60, 71–83.
Dogan, I., et al., 2009. Multiple layers of B cell memory with different effector functions. Nat. Immunol. 10, 1292–1299.
Duddy, M., et al., 2007. Distinct effector cytokine profiles of memory and naive human B cell subsets and implication in multiple sclerosis. J. Immunol. 178, 6092–6099.
Feske, M.L., Medina, M., Graviss, E.A., Lewis, D.E., 2012. In: Kalyuzhny, A.E. (Ed.), Handbook of ELISPOT: Methods and Protcocols, vol. 792. Humana Press, pp. 229–241, chap. 18.
Fleming, J.O., Trousdale, M.D., el-Zaatari, F.A., Stohlman, S.A., Weiner, L.P., 1986. Pathogenicity of antigenic variants of murine coronavirus JHM selected with monoclonal antibodies. J. Virol. 58, 869–875.
Geffroy-Luseau, A., et al., 2011. TLR9 ligand induces the generation of CD20+ plasmablasts and plasma cells from CD27+ memory B-cells. Front. Immunol. 2, 83.
Greicius, G., Severinson, E., Beauchemin, N., Obrink, B., Singer, B.B., 2003. CEACAM1 is a potent regulator of B cell receptor complex-induced activation. J. Leukoc. Biol. 74, 126–134.
Hawkins, E.D., et al., 2013. Quantal and graded stimulation of B lymphocytes as alternative strategies for regulating adaptive immune responses. Nat. Commun. 4, 2406.
Hebeis, B.J., et al., 2004. Activation of virus-specific memory B cells in the absence of T cell help. J. Exp. Med. 199, 593–602.
Henn, A.D., et al., 2009. Modulation of single-cell IgG secretion frequency and rates in human memory B cells by CpG DNA, CD40L, IL-21, and cell division. J. Immunol. 183, 3177–3187.
Jacobi, C., Lange, P., Reiber, H., 2007. Quantitation of intrathecal antibodies in cerebrospinal fluid of subacute sclerosing panencephalitis, herpes simplex encephalitis and multiple sclerosis: discrimination between microorganism-driven and polyspecific immune response. J. Neuroimmunol. 187, 139–146.
Jahnmatz, M., et al., 2013. Optimization of a human IgG B-cell ELISpot assay for the analysis of vaccine-induced B-cell responses. J. Immunol. Methods 391, 50–59.
Küppers, R., 2008. Human memory B cells: memory B cells of a special kind. Immunol. Cell Biol. 86, 635–636.
Kapoor, H., et al., 2004. Persistence of West Nile Virus (WNV) IgM antibodies in cerebrospinal fluid from patients with CNS disease. J. Clin. Virol. 31, 289–291.
Karulin, A.Y., Lehmann, P.V., 2011. In: Kalyuzhny, A.E. (Ed.), Handbook of ELISPOT: Methods and Protocols, vol. 792. Humana press, pp. 125–143, chap. 11.
Khairnar, V., et al., 2015. CEACAM1 induces B-cell survival and is essential for protective antiviral antibody production. Nat. Commun. 6, 6217.
Klein, U., Rajewsky, K., Küppers, R., 1998. Human immunoglobulin (Ig)M+IgD+ peripheral blood B cells expressing the CD27 cell surface antigen carry somatically mutated variable region genes: CD27 as a general marker for somatically mutated (memory) B cells. J. Exp. Med. 188, 1679–1689.
Kometani, K., et al., 2013. Repression of the transcription factor Bach2 contributes to predisposition of IgG1 memory B cells toward plasma cell differentiation. Immunity 39, 136–147.
Krumbholz, M., Derfuss, T., Hohlfeld, R., Meinl, E., 2012. B cells and antibodies in multiple sclerosis pathogenesis and therapy. Nat. Rev. Neurol. 8, 613–623.
Kurosaki, T., Kometani, K., Ise, W., 2015. Memory B cells. Nat. Rev. Immunol. 15, 149–159.
Lin, M.T., Hinton, D.R., Marten, N.W., Bergmann, C.C., Stohlman, S.A., 1999. Antibody prevents virus reactivation within the central nervous system. J. Immunol. 162, 7358–7368.
Linnoila, J.J., Binnicker, M.J., Majed, M., Klein, C.J., McKeon, A., 2016. CSF herpes virus and autoantibody profiles in the evaluation of encephalitis. Neurol. Neuroimmunol. Neuroinflamm. 3, e245.
Lino, A.C., Dörner, T., Bar-Or, A., Fillatreau, S., 2016. Cytokine-producing B cells: a translational view on their roles in human and mouse autoimmune diseases. Immunol. Rev. 269, 130–144.
Liu, A.H., Jena, P.K., Wysocki, L.J., 1996. Tracing the development of single memory-lineage B cells in a highly defined immune response. J. Exp. Med. 183, 2053–2063.
Lund, F.E., 2008. Cytokine-producing B lymphocytes-key regulators of immunity. Curr Opin. Immunol. 20, 332–338.
Marques, C.P., et al., 2011. CXCR3-dependent plasma blast migration to the central nervous system during viral encephalomyelitis. J. Virol. 85, 6136–6147.
Metcalf, T.U., Griffin, D.E., 2011. Alphavirus-induced encephalomyelitis: antibody-secreting cells and viral clearance from the nervous system. J. Virol. 85, 11490–11501.
Metcalf, T.U., Baxter, V.K., Nilaratanakul, V., Griffin, D.E., 2013. Recruitment and retention of B cells in the central nervous system in response to alphavirus encephalomyelitis. J. Virol. 87, 2420–2429.
Michel, L., et al., 2015. B cells in the multiple sclerosis central nervous system: trafficking and contribution to CNS-compartmentalized inflammation. Front. Immunol. 6, 636.
Niino, M., Hirotani, M., Miyazaki, Y., Sasaki, H., 2009. Memory and naive B-cell subsets in patients with multiple sclerosis. Neurosci. Lett. 464, 74–78.
Pape, K.A., Taylor, J.J., Maul, R.W., Gearhart, P.J., Jenkins, M.K., 2011. Different B cell populations mediate early and late memory during an endogenous immune response. Science 331, 1203–1207.
Phares, T.W., DiSano, K.D., Stohlman, S.A., Bergmann, C.C., 2014. Progression from IgD+ IgM+ to isotype-switched B cells is site specific during coronavirus-induced encephalomyelitis. J. Virol. 88, 8853–8867.
Phares, T.W., DiSano, K.D., Stohlman, S.A., Segal, B.M., Bergmann, C.C., 2016. CXCL13 promotes isotype-switched B cell accumulation to the central nervous system during viral encephalomyelitis. Brain Behav. Immun. 54, 128–139.
Pinna, D., Corti, D., Jarrossay, D., Sallusto, F., Lanzavecchia, A., 2009. Clonal dissection of the human memory B-cell repertoire following infection and vaccination. Eur. J. Immunol. 39, 1260–1270.
Ridderstad, A., Tarlinton, D.M., 1998. Kinetics of establishing the memory B cell population as revealed by CD38 expression. J. Immunol. 160, 4688–4695.
Sanz, I., Wei, C., Lee, F.E., Anolik, J., 2008. Phenotypic and functional heterogeneity of human memory B cells. Semin. Immunol. 20, 67–82.
Shimoda, M., Koni, P.A., 2007. MHC-restricted B-cell antigen presentation in memory B-cell maintenance and differentiation. Crit. Rev. Immunol. 27, 47–60.
Sibley, L.S., et al., 2012. ELISPOT refinement using spot morphology for assessing host responses to tuberculosis. Cells 1, 5–14.
Skoldenberg, B., Kalimo, K., Carlstrom, A., Forsgren, M., Halonen, P., 1981. Herpes simplex encephalitis: a serological follow-up study. Synthesis of herpes simplex virus immunoglobulin M, A, and G antibodies and development of oligoclonal immunoglobulin G in the central nervous system. Acta Neurol. Scand. 63, 273–285.
Slifka, M.K., Ahmed, R., 1996a. Long-term humoral immunity against viruses: revisiting the issue of plasma cell longevity. Trends Microbiol. 4, 394–400.
Slifka, M.K., Ahmed, R., 1996b. Limiting dilution analysis of virus-specific memory B cells by an ELISPOT assay. J. Immunol. Methods 199, 37–46.
Slifka, M.K., Antia, R., Whitmire, J.K., Ahmed, R., 1998. Humoral immunity due to long-lived plasma cells. Immunity 8, 363–372.
Tangye, S.G., Hodgkin, P.D., 2004. Divide and conquer: the importance of cell division in regulating B-cell responses. Immunology 112, 509–520.
Tangye, S.G., Liu, Y.J., Aversa, G., Phillips, J.H., de Vries, J.E., 1998. Identification of functional human splenic memory B cells by expression of CD148 and CD27. J. Exp. Med. 188, 1691–1703.
Taylor, J.J., Pape, K.A., Jenkins, M.K., 2012. A germinal center-independent pathway generates unswitched memory B cells early in the primary response. J. Exp. Med. 209, 597–606.
Thomson, S., 2005. Methods in molecular biology, volume 302: handbook of elispot: methods and protocols. Immunol. Cell Biol. 83, 586-586.
Tomayko, M.M., Steinel, N.C., Anderson, S.M., Shlomchik, M.J., 2010. Cutting edge: hierarchy of maturity of murine memory B cell subsets. J. Immunol. 185, 7146–7150.
Tschen, S.I., et al., 2002. Recruitment kinetics and composition of antibody-secreting cells within the central nervous system following viral encephalomyelitis. J. Immunol. 168, 2922–2929.
Vences-Catalán, F., Santos-Argumedo, L., 2011. CD38 through the life of a murine B lymphocyte. IUBMB Life 63, 840–846.
Walsh, P.N., et al., 2013. Optimization and qualification of a memory B-cell ELISpot for the detection of vaccine-induced memory responses in HIV vaccine trials. J. Immunol. Methods 394, 84–93.
Wang, F.I., Hinton, D.R., Gilmore, W., Trousdale, M.D., Fleming, J.O., 1992. Sequential infection of glial cells by the murine hepatitis virus JHM strain (MHV-4) leads to a characteristic distribution of demyelination. Lab. Invest. 66, 744–754.
Williams, R.K., Jiang, G.S., Snyder, S.W., Frana, M.F., Holmes, K.V., 1990. Purification of the 110-kilodalton glycoprotein receptor for mouse hepatitis virus (MHV)-A59 from mouse liver and identification of a nonfunctional, homologous protein in MHV-resistant SJL/J mice. J. Virol. 64, 3817–3823.
Xiao, Y., Hendriks, J., Langerak, P., Jacobs, H., Borst, J., 2004. CD27 is acquired by primed B cells at the centroblast stage and promotes germinal center formation. J. Immunol. 172, 7432–7441.
Zuccarino-Catania, G.V., et al., 2014. CD80 and PD-L2 define functionally distinct memory B cell subsets that are independent of antibody isotype. Nat. Immunol. 15, 631–637.